Modern approach to surface layer modifications of hydrated cement paste for improving permeability estimates of virtual concrete

Piet Stroeven [1], Kai Li [2]

[1] Delft University of Technology, Faculty of Civil Eng. and Geosciences, the Netherlands

[2] Hunan University, College of Civil Engineering, Changsha, China (kaili@hnu.edu.cn)

Permeability estimates obtained by physical experiments and by simulations differ quite significantly. When biases at the experimental side would be eliminated, the expected modest gap could be bridged by surface layer modifications of the hardened cement paste, discussed herein. This involves the formation of a fractal-like nano-particle structure in the outer hydration layer, instead of the smooth-surfaced layer obtained by the vector approach. This study firstly applies a DLA method for simulating the fractal structure of nodules in a low-density 2D setting of mono-size cement particles. Herewith it is confirmed that density of the outer hydration layer will diminish almost linearly away from the inner one, inevitably leading to permeability decline. This approach yielded also a realistic range of modifications for the outer layer, *i.e.*, a 0.1 to 0.5 μm increased thickness. Therefore, in the normal 3D set up, the smooth vector-based hydration layer is given a stepwise thickness increase in this range, whereupon the consequences for pore geometry and topology, as well as for permeability can be investigated. The outcomes of this study are laid down in a separate publication. When further *structural* information on nano level will become available in the near future, the simulations can be appropriately adapted. This paper specifically proposes as a practical methodology to slightly step-wise enlarge at the packing simulation stage the *fresh cement grains* in proportion to their respective sizes. The herein introduced standard methodology for porosimetry and permeability estimation can readily be employed for simulating these cases. This is demonstrated for cement paste with *w/c* = 0.5, whereby packing density is increased by about 1% per step. This can be associated with a fictitious reduction in *w/c* from 0.49 to 0.45. It could be demonstrated this way that a permeability decline of one order of magnitude can be realized, *i.e.*, at least enough to bridge the modest gap with corrected experimental permeability data. So, the final solution can be expected in this range.

Keywords: Cement, hydration, surface modification, nano-packing, permeability, simulation

1 Introduction

Because of economic reasons, cementitious materials are nowadays simulated by computer. The prime engineering representative "concrete" is thereby denoted "compucrete". Although this most widely employed construction material is frequently treated as a strong substance that properly serves in engineering environments for long periods of time, deterioration will nevertheless earlier or later take place. Concrete's positive qualification is due to the hydrating cement paste that fills up the voids between a wide range of aggregate particles (sand and gravel) that are mostly highly durable itself. Nevertheless, capillary porosity is developing during this hardening process. Capillary pores that can transmit fluids through the material that will give rise to corrosion of the reinforcement and to freeze-thaw damage. Harmful substances in the fluid may deteriorate the material as well. Hence, studies of permeability are highly relevant. The most popular experimental approach is mercury intrusion porosimetry (MIP), providing the bulk of information for validating virtual approaches, however demonstrated leading to significantly biased information (Diamond, 2000).

Making virtual cementitious materials is accomplished in our case by the discrete element method (DEM), although random sequential addition (RSA) is by far more popular in concrete technology. DEM provides a higher packing capacity and the resulting particle dispersion is more realistic (Li and Stroeven, 2018). And even significantly better than realized by completely randomized systems (Garboczi and Bentz, 2001). In our previous studies, DEM was first employed to study compacted aggregate particles with different shapes (He, *et al*. 2010). For representativeness, containers should be 5 times larger than aggregate's maximum grain size. Hence, operation is situated on *decimetre* level and aggregate grains itself are measured in *centimetres*, which is the *meso-level* of research. As for the fresh cement mixture, involving a wide range of grain sizes (1 to 100 μm), investigations are on *micro-level*. However, the range is narrowed for simulation purposes. Moreover, the observed angular shape of cement grains (Garboczi and Bullard, 2004) is neglected when hydration simulation is performed. The hydrating and as a consequence expanding particles lead to complicated and thus very time-consuming interference problems when non-spherical shapes are considered. Hydration simulation can therefore be accomplished by a vector approach, eXtended Integrated Particle Kinetics Method

(XIPKM) (Le, *et al*. 2013). This is a more realistic extension of the well-known IPKM (Bishnoi and Scrivener, 2009). So, hydrated particles are spherical and have a smooth surface in virtual reality. The hydrated material incorporates a complex and highly irregular system of capillary pores. This is *the subject matter of engineering interest*. Figure 1 shows the pore system when the surrounding solid material is removed.

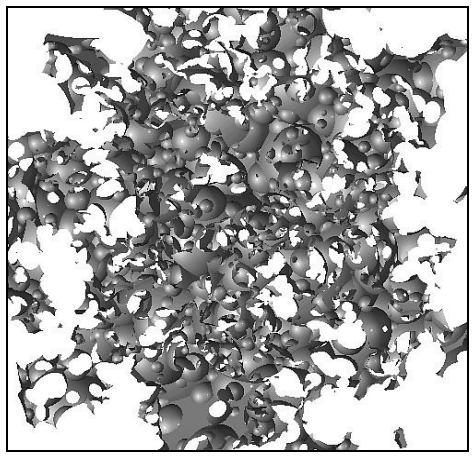

Figure 1. Capillary pore system in hardened cement paste (after removal of the solid component) (w/c = 0.26; 10 years of hydration)

A porosimetry concept is derived from the rapidly exploring random tree (RRT) system in robotics (LaValle and Kuffner, 2001). The resulting double random multiple-tree structuring (DRaMuTS) is employed to explore the pore system by traversing all pores, leading to a tree-like pore network structures, of which the main channels are of engineering relevance. They meander throughout container space, even when aggregate surfaces would be close by, so that interfacial transition zones (ITZs) develop, which are supposed being more porous than bulk material. Pore size in such a highly irregular system (which also holds for *shape*) is obtained by star volume measuring (SVM) in a very large number of points dispersed uniformly at random (UR) in pore space (Stroeven, 2019). This method was successfully employed in life science research (Gundersen, *et al*. 1988). Finally, information on location and size of main channels is used in a so-called traditional network approach to estimate permeability (Stroeven, *et al*. 2015). The influence of pore shape is incorporated as well. The conductance decline with respect to a circular section is assessed for that purpose by finite element analysis (FEA) (Le, 2015).

This are the contours of the regular approach to permeability estimation by virtual cementitious materials. Though biased, experimental data seem to be pointing to lower permeability in reality. When biases due to non-saturated samples are considered and the transfer is made from cement paste in simulations to concrete that is used in most experiments, only a modest gap (one order of magnitude) is resulting in permeability. This could be bridged by the 'surface layer modifications' to be discussed in this paper.

To bridge this gap, the so-called outer deposition layer of the main hydration product – calcium silicate hydrate (C-S-H) – is considered packed by nano-particles in conformity with experimental observations (Jennings, 2008). Hence, we are herewith going down from *micro*- into the *nano*-level of materials. So, instead of a smooth-surfaced layer due to the vector approach, a supposedly thicker rough-surfaced C-S-H layer is obtained, yielding a reduction in median pore size and in pore connectivity. This paper concentrates on these latest aspects of our adventures into concrete structure. The most practical problem of estimating the reduction in the traditional way determined water permeability characteristics – on micro-level – is basically solved. The resulting decline in permeability of the cement paste can be combined with the dilution and tortuosity effects in the concrete to estimate concrete permeability. Results are coming as a consequence closer to experimental data. A second problem has not been approached yet. It concerns the porosimetry and permeability estimation of the nano-structured outer hydration layer. However, expectation is that the traditional approach of DRaMuTS and SVM will be applicable to the nano-system. Major drawback in both cases is that the *spatial structure of globules dispersion* is as yet unknown (Nguyen, 2014). The approximate character of the solution of our prime problem is therefore due to this lacking information.

2 Standard approach to porosimetry and permeability estimation

DEM initially distributes particles (*e.g.* by RSA procedure) in an enlarged container (Fig. 2, left). Next, particles are set to move, while at the same time the container size is reduced. Realization of inter particle contacts and contact of particles with boundaries is part of the DEM system. When the required particle density is obtained (Fig. 2, right), the generation procedure is terminated. Particles can also be non-spherical. In that case, particles are undergoing a linear movement and a rotation. For further details, see (He, *et al*. 2012; O'Connor, 1996; Williams and Philipse, 2003).

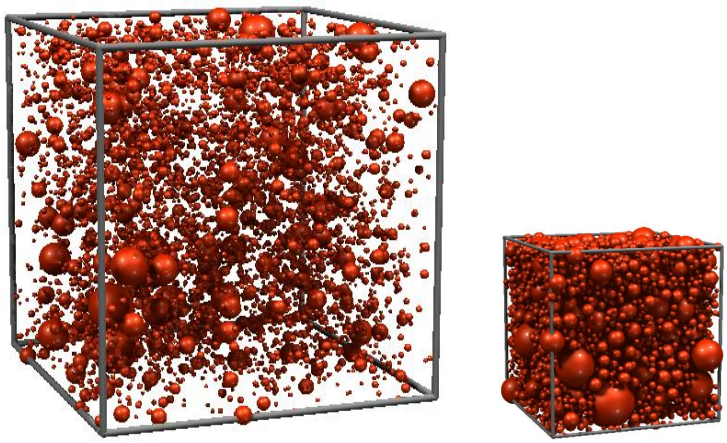

Figure 2. (left) Start of the production process by DEM of particle mixture dispersed in an enlarged container. (right) After gradual size reduction of the container the dynamic process stops at the required density.

The packed particle mixture of (blended) Portland cement grains, is hydrated in accordance with XIPKM, transforming it gradually into a hardened virtual material (Fig. 3). For specific details, see (Le, *et al*. 2013). Figure 3 explicitly reveals the outer hydration layer of the hydrated cement particles (*i.e.* CSH-out). This is the prime subject matter discussed later on.

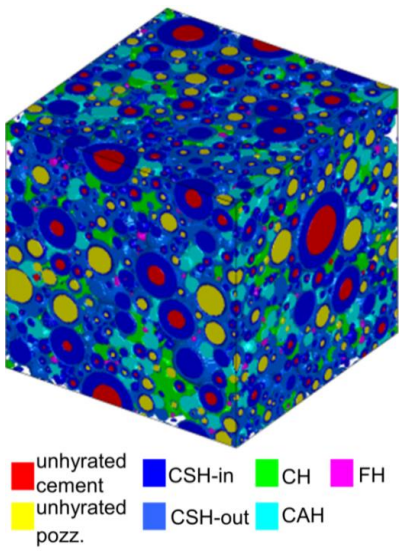

Figure 3. Colour coded virtual hydrated blended Portland cement paste

The hydration simulation finally produces also a complex and tortuous pore network system as already depicted in Figure 1. This is targeted by DRaMuTS (Le, 2015; Le, *et al*. 2013). Nodes are for that purpose uniformly random distributed in the virtual material. Basically, the nodes in pore space are connected by straight lines. Only when this line intersects with the pore surface, the node is shifted along the line to avoid intersections, however violating the UR state. Tree-like structures are developed in this way of which neighbouring trees connect when located in the same pore channel. Topology of this pore network is analysed and main channels (connecting opposite free surfaces) are distinguished from branching dead-end pores and isolated ones, as displayed in Figure 4. The zigzag shaped tree channels are finally smoothed by a mathematical operation.

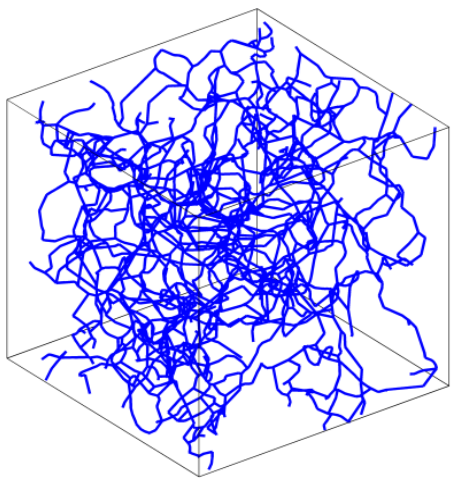

Figure 4. Main pore channels meandering in container space (w/c = 0.4, Blaine surface area is 300 m²/kg and porosity is 19%). Four rigid sides and two free surfaces at the top and bottom of cube.

Pore geometry is obtained by SVM (Le and Stroeven, 2012; Stroeven, 2020). For that purpose, a new UR node system is superimposed on the virtual material of which only the nodes in pore space are employed. The fraction of nodes in the pores governs porosity. Next, all nodes in the pores are provided with 3D stars to determine the size of the local representative sphere (having the same volume as the pore locally has) (Stroeven, 2020). This allows constructing a volume-based pore size distribution function. Alternatively, all nodes in pores are provided with 2D stars in an isotropic uniformly random (IUR) set of pore sections. This renders possible determination of a series of representative circles in the

respective sections. The smallest among them determines the pore throat size that is used in the next operation.

Finally, a traditional network structure is constructed on the basis of the nodes and cylindrical pore sections of associated throat sizes. Shape effects on conductance is accounted for by FEA of a large number of throats. This configuration is subjected to water pressure on the parallel free surfaces. A system of n equations with n unknowns is resulting. Solution leads to information on the global permeability of this pore system. For more information, see (Le, 2015).

3 DLA-based simulation of rough surface layer in 2D

Since all particles are simplified as spheres in XIPKM, their surfaces are presumed to be uniform and smooth. However, this assumption is in conflict with experimental observations (Gartner, *et al*. 2000). A fractal-like structure of C-S-H is observed indicating that a rough surface should be produced in the hydration model. Jennings proposed a model of spherical globules of 5 nm (Jennings, 2000). The debate on the structure of C-S-H in concrete is however still ongoing. A simple generation process was therefore designed for our limited goals, pursuing the rough estimation of pore size reduction by replacing the standard uniform outer hydration layer for a nano-scale fractal-like structure of connected globules. Also, the unknown 3D characteristics of this on nano-level structured surface layer did not warrant doing this generation in 3D. Instead, a diffusion limited aggregation (DLA) model – used in chemistry research – has been implemented for hydration simulation of the fractal-like structure of C-S-H. Complex hydration mechanisms are neglected in this stage of modelling. Periodic boundaries are used to eliminate any edge effects on the simulated structure.

Specifically, the C-S-H in this outer layer is treated as an inhomogeneous material consisting of small spherical nano-size globules in accordance with Jennings' model. Upon starting the hydration process, the produced C-S-H dissolves in water and nucleates in open pore space to form globules with a certain size. Then, these globules are assigned with random velocities and transferrable directions, providing for their free movement in the system. All cement grains are fixed as seed particles on micro-level. Hence no movements are allowed. The growth of C-S-H always starts from the surface of cement grains' inner hydration layer, which is in conformity with experimental observations

(Gartner, *et al*. 2000). If overlaps between globules and seed particles are detected, these globules will immediately stick to the grains and become new immobile seed particles. The simulation is controlled by the cycle of iterations, and the process terminates when the number of moving globules in the system is exhausted. In this way, the fibrous structure of C-S-H can be well represented. As stipulated, the developed DLA model can only be applied in 2D simulations, because the number of globules required in a 3D simulation will exceed normal computational capabilities. Figure 5 is an illustration in which the hydrate structure generated by the traditional vector-based model and by the DLA approach are compared. The influence of the structural changes in hydrated cement paste on porosimetry outcomes and permeability data will be discussed later.

4 Results in 2D setting

4.1 Simulation

The DLA model was implemented in the hydration simulation stage to generate fibrous C-S-H, as illustrated in Figure 6. Although cement grains in practice have irregular shape (Garboczi and Bullard, 2004) and a certain size range (1-100 μm), they are simplified as disk-like particles of 2 μm in size to ensure the computational efficiency. For the same reason, the globules are assumed mono-size and their size is set as 50 nm which is almost ten times larger than the reported value in Jennings' colloid model (Jennings, 2000; Jennings, 2008). The size of the container in the simulation is 25 μm. The globule/container

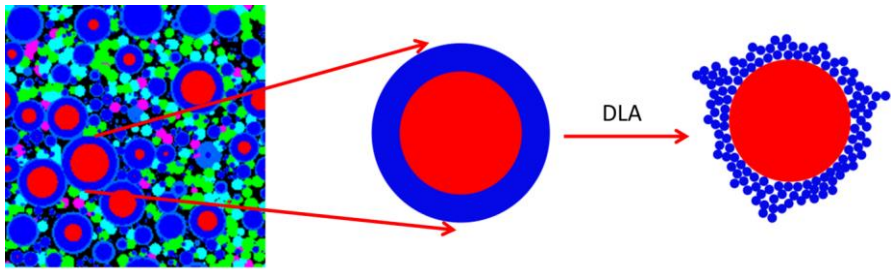

Figure 5. (a) Example of 2D section of hydrated plain cement paste; pore space in black; (b) Illustration of a hydrating cement particle in XIPKM. Red: unhydrated nucleus and the inner C-S-H layer; blue: the outer C-S-H layer. (c) Implementation of the DLA algorithm in XIPKM leads to an inhomogeneous C-S-H outer layer. The other compounds of cement paste are neglected in this 2D illustration image.

size ratio is important, because representative data can only be obtained when the ratio is large enough (Stroeven, *et al*. 2010). However, the same results are obtained for 5 nm globules in a 2.5 µm container and 0.2 µm cement grains. The low-volume mixture is designed to just render possible better visualizing the effects of nano-aggregation. Realistic would be a 70% reduced average inter-particle distance. *However, the structural effects of expansion of the hydrated cement particles and roughening of their surfaces due to the nano-particle surface layer modification process are evident.*

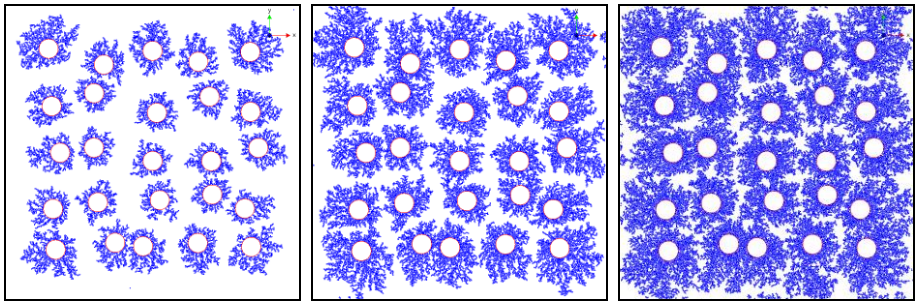

Figure 6. Three successive hydration stages obtained by DLA modelling in 2D. Red circles represent the disk-like cement grains (also involving the inner hydration layer) while blue ones indicate the C-S-H globules. CH is not taken into account in this case.

It is confirmed that the growth of C-S-H starts from the surface of the cement particles, and then gradually fills in the available pore space. The three successive stages in Figure 6 indicate the structural developments of the maturing paste. Due to the low-volume setting, the "fractal-like arms" of nano-particles from neighbouring cement particles do not significantly interfere. Obviously, pore space is reduced during hydration. A report on a more extensive study is planned for a future publication.

Figure 7 shows the morphological differences between 2D simulated structures generated by XIPKM and DLA, respectively. *The total amount of C-S-H is the same in both cases*. The thickness of outer C-S-H layer is around 0.95 µm in Figure 7a; the number of nano-globules in Figure 5b is 36000. The fibrous nano-level growth will yield smaller pores. This is confirmed by results presented in Figure 8, since an obvious shift to the left in pore size distribution is found. Moreover, the rough surface caused by the fibrous structure also leads to a reduction in connected pores. As already shown in (Ye, 2005), declining pore size and connectivity of capillary pores mitigate the fluid transport process and thus lead to lower permeability. This will be discussed in the next section.

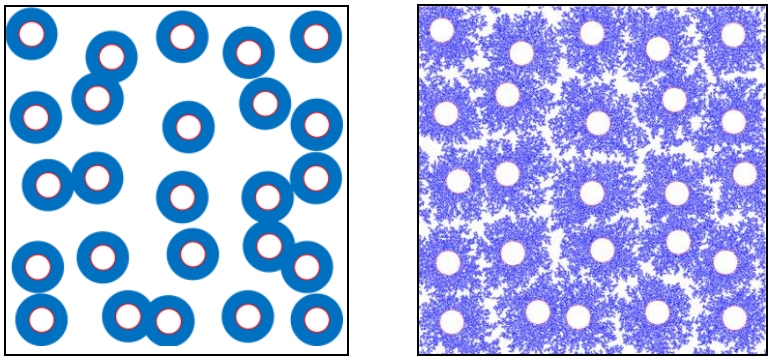

Figure 7. The structure of cement paste in 2D consisting of DEM-packed mono-size cylindrical disks under two different growth mechanisms: (left) homogenous expansion; (right) fibrous growth by aggregation of mono-size globules up to stage 3 (whereby fibrous arms are not significantly interfering). Amount of C-S-H in both cases is kept the same. The centrally located particle in the second layer from the top is quantitatively evaluated as to gradient in density, as shown also in (Li and Stroeven, 2021).

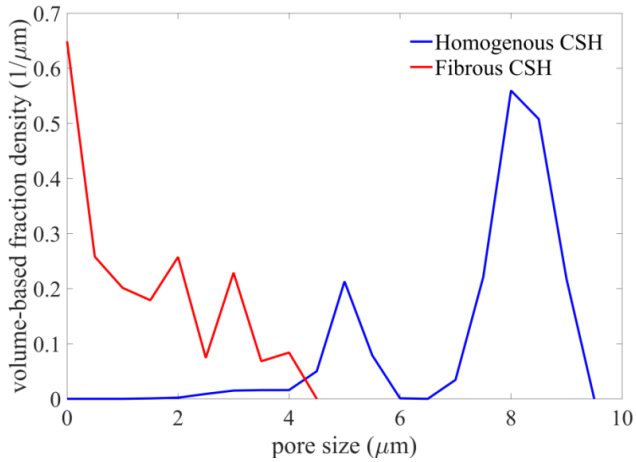

Figure 8. 2D PSD due to homogenous expansion (Fig. 7a) and fibrous growth (Fig. 7b)

4.2 ***Properties of globular layer***

To get a more quantitative idea of the consequences of replacing the homogeneous outer hydration layer by a layer of fractal-like clusters of globules, the central particle in the second row from the top in Figure 7 (right) is quantitatively analysed. To that end, the 2 μm section of the cement particle was enlarged to 70 mm, implying a scale factor δ of $70000/2 = 35\times10^3$. The resulting picture of the rough surface layer is depicted in Figure 9. It

was analysed by line scanning method, in this case in the form of equidistant circles. The intersected number of objects, N_o, as well as the number of void places, N_v, was determined. Obviously, $N_o/(N_o+N_v) = A_A$. Hence, areal fraction A_A, and thus volume fraction V_V, is readily obtained. Along the first circle, adjacent the cement grain section, we have 106/157 = 0.67 = A_A, which corresponds well with the assumed density in the homogeneous outer hydration layer.

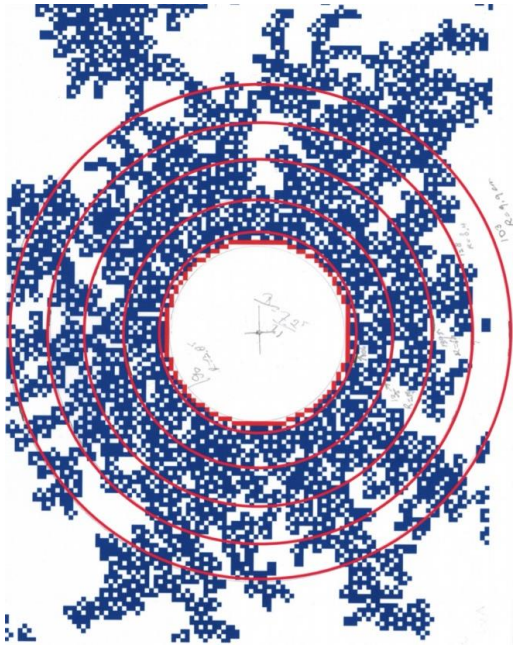

Figure 9. Major part of the DLA-produced globular structure (displayed around the central particle in the second row from the top in Figure 7). Diameter of grain section (+ inner hydration layer) amounted 7 mm during application in this working document of lineal analysis with concentric equidistant circles.

The five circles are located 0.12, 0.57, 1.02, 1.47 and 1.92 µm away from the inner layer of the hydrated cement grain, respectively. With L as the length of the circle, we have assessed the values of $N_o/L = N_L$ per circle. The values collected in Table 1 were obtained. An almost linear decline in N_L is observed, so that *the rough surface layer is always thicker than the uniform layer*, because originally assumed having a constant density with areal (and volume) fraction of 0.64. The thickness of the homogeneously expanded outer hydration layer in Figure 7 (left) is approximately 0.95 µm. Hence, circles 3 to 5 are on larger distances. In 3D, the location of the surface of the rough layer will therefore be located

Table 1. Results of scanning operation displayed in Figure 9

Circle	N_L (mm^{-1}) in enlarged picture	N_L (μm^{-1}) on real scale	Volume fraction V_V
1	0.432	12.3	0.67
2	0.398	11.4	
3	0.321	9.2	
4	0.243	7.0	
5	0.166	4.7	0.22

between 1 to 1.5 μm away for the centre of this hydrated grain with a radius of (1 + 0.95) μm. When the globular layer would expand to 1.2 μm outside the (approximately) 1 μm outer hydration layer, we have for the volume of globules (= volume particles in hydrated layer): $V = 0.64 \times \pi\ (23 - 13)/6 \approx 0.5 \times \pi\ (2.23 - 1)/6 \approx 0.6$ μm^3, where volume fraction at 1.2 μm was declined to 0.45. Herein, we have assumed the density decline in 3D roughly similar to that in 2D.

Yet, the large range of particle sizes involved and the higher packing density in real cement paste will complicate matters. However, the expansion of the nano-packed outer hydration layer should ultimately be assessed by 3D packing simulation tests based on more realistic structural features that are as yet unknown. The 2D set up is selected because even a simplified set up of the particle-packed nano-structure would be outside present computational capabilities. Still, the selected approach yields some insight on a possible range of expansions. This range of 0.1 μm to 0.5 μm is taken large enough to incorporate future practical solutions based on *forthcoming structural information*.

5 Implementation in 3D

The effects on various properties of nano-particle structure formation in the outer hydration layer are elaborated in a publication in progress. Herein, as a first trial, the thickness of the C-S-H layer obtained after simulation by XIPKM is successively *for each particle* enlarged by 0.1 μm, 0.2 μm, 0.3 μm, 0.4 μm and 0.5 μm (denoted as the thickness of the rough surface layer), while maintaining the other details of the setup. Note that there are no changes in the size of CH during hydration simulation. We have seen in the 2D case that this is a wide range of thickness increases that will surely incorporate the practical solution. This is convincingly demonstrated by the dramatic drop in water permeability (from 10^{-15} m^2 to 10^{-19} m^2) over the investigated range as shown in Figure 10. Hence, the

expected solution (one order of magnitude drop in permeability) should be located in the first part of the range. This will be discussed in the next section.

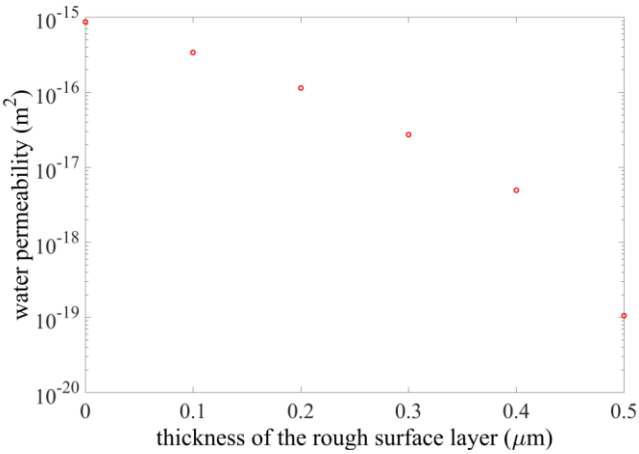

Figure 10. Water permeability as a function of the thickness of the rough surface layer

6 Direct approach to the surface modification case

In the densely packed multi-size cement grain structure, hydration of the outer hydration layer will be the result of a packing process of nano-size globules around all cement particles, yielding fractal-like arms mutually penetrating in the open space left at that moment by arms of neighbouring hydrating cement particles. The major part of this situation could even be simulated *at present day* by having the cement particles hydrating in the DEM-packed state of the cement grains (in accordance with the required *w/c* ratio) with slightly upgraded hydration parameters yielding somewhat enlarged hydrated particles (supposedly *proportional to the cement particle's size*). This could readily be achieved by an upgraded version of XIPKM. In this concept, the "rough surface layer" would be *integrated* in the smooth-surfaced body of the outer hydration layer. The percentage extra growth of all cement particles could be step-wise varied as in the present paper. Also, porosimetry and permeability assessment will be similar. *Just the conductance reduction by surface roughness would be missing*.

However, the *same situation* could be obtained for a given cement paste upon stepwise slightly increasing the density of the DEM-packed *fresh* cement grain mixture (thus, quasi reducing step-wise the *w/c* ratio), and thereupon following the standard methodology for hydration (XIPKM), porosimetry (DRaMuTS and SVM) and permeability assessment

(network analysis). In both cases, validation with reliable experimental data will still be troublesome because of the biased nature of the majority of experimental approaches. Figure 11 may illustrate this approach. The development in permeability with the degree of hydration (DOH) is herein depicted for mixes with *w/c* ratios of 0.4 and 0.5, respectively. Comparison learns that at, *e.g.*, DOH = 0.7, the permeability in bulk material drops by about *two orders of magnitude* when the *w/c* ratio is reduced from 0.5 to 0.4. Hence, even when the *w/c* ratio would be stepwise modified (*i.e.* the associated cement packing density appropriately increased) by 0.01 to 0.05 (so, starting by *w/c* = 0.5 going down to *w/c* = 0.45), we would be able covering a permeability change of *one order of magnitude*! At *w/c* = 0.5, the cement takes 39% of the total volume, at *w/c* = 0.4 this increases to 45%. Hence, density would be increased by roughly 1% per step. Note that the results in Figure 11 are from (Li, 2017; Li, *et al*. 2017).

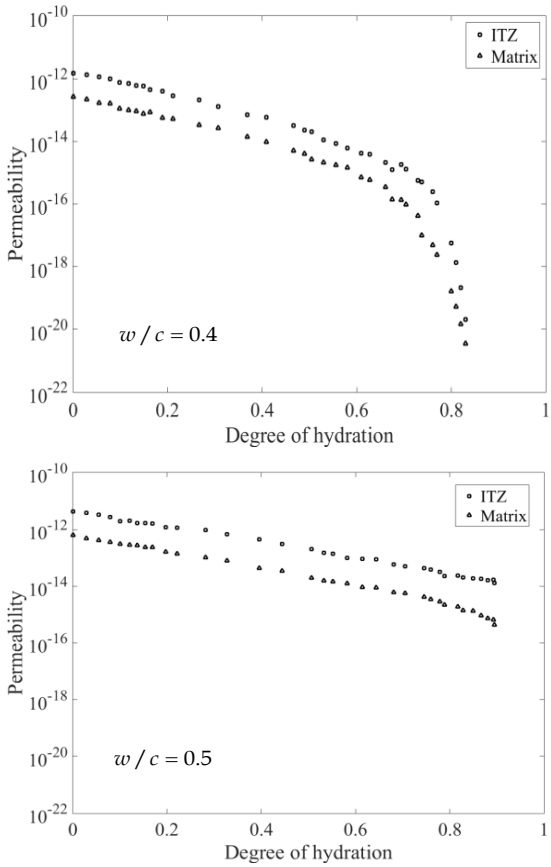

Figure 11. Permeability of ITZ and matrix material versus the degree of hydration (DOH) at w/c = 0.4 (top) and 0.5 (bottom) (Li, 2017)

7 Discussion

In our standard 3D methodology for porosimetry, the outer hydration layer's density is uniformly distributed and the free surface is smooth. Yet, relatively new is the understanding that nano-packing is involved. So far, the traditional 3D approach has assumed the loose random nano-packing state (volumetric ratio of 0.64) to govern the structure of the outer layer. In agreement with the international literature (Jennings, 2000), a more fractal-like structure of globules should be considered that may reduce pore space and thus permeability. More detailed information on the structural details is unfortunately still missing.

A 2D set up was considered in this situation an economic way to *qualitatively* analyse structural modifications by nano-packing and the consequences for permeability. When the most practical case of the ultimate hydration degree is selected, one could expect the inner part of the outer hydration layer's volumetric density to be on average around 0.64. The 2D image analysis results presented herein (obtained by lineal analysis: Rosiwal, 1898; Underwood, 1967; Stroeven and Hu, 2006) revealed a value quite close by (*i.e.* 0.67). Hence, a thickness increase of this outer layer will be in the first place due to the declining density value away from the inner hydration layer's surface. So, the remaining pore space will have declined, reducing permeability. Finally, the rough pore surface will additionally diminish water transport. This is a common feature faced in transport of water through pipes with a certain surface roughness (Zhang, *et al*. 2019). The latter effect is not quantified in this paper, since 3D simulation results are required to see how nano-particle interferences will influence surface roughness.

Finally, the situation at the moment does not render possible validating an upgraded numerical estimate for permeability. Le determined permeability by the herein discussed standard methodology for various cement mixtures (Le, 2015); data for w/c = 0.4 were close to those of Li presented in Figure 11 at the bottom. Experimental data of similar PC pastes obtained by Odler and Köster (1991) and by Banthia and Mindess (1989) yield three orders of magnitude lower values, *i.e.* 2.8×10^{-18} and 10^{-18}.

These examples represent the actual state of affairs. Moreover, it should be mentioned that the bulk of permeability research data are traditionally obtained by most popular MIP method in concrete technology. This yields however almost two orders of magnitude

biased results as compared to image analysis studies (Diamond, 2000). All the specimens selected in this study are fully saturated with water, as assumed in most experimental approaches. Yet, it has been shown in the literature that even in case of underwater storage, the fully saturated state assumed in the experimental studies cannot be achieved (Zalzale, 2013; Muller, *et al*. 2013). This is required however to use Darcy's formula for deriving permeability in a pore network analysis. The pastes in real situations are generally partially saturated. Still, even modest deviations from the state of full saturation have been shown significantly reducing permeability (Kameche, *et al*. 2014; Li, *et al*. 2019). This is depicted in Figure 12. This effect closes *also* part of the gap between permeability data derived from virtual and real cement-based materials. Note that the data on cement paste have to be transferred to concrete used in most of the experimental set ups. This is readily achieved by accounting for the aggregate's dilution and tortuosity effects in the concrete (Li, *et al*. 2017).

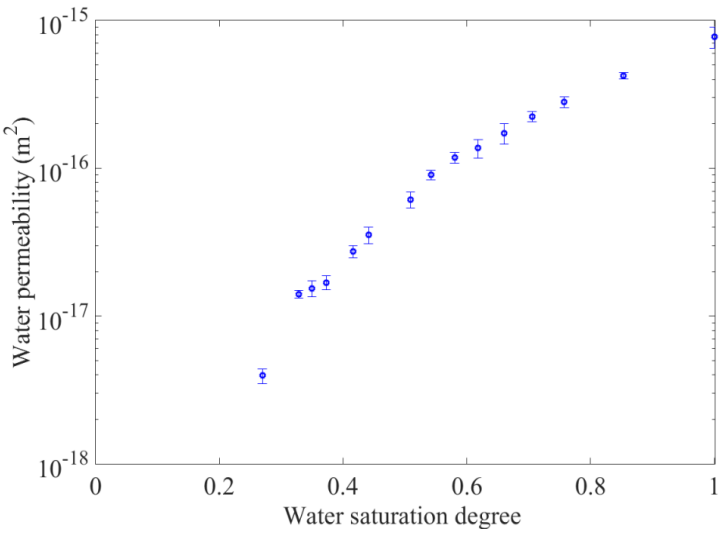

Figure 12. Effect of the saturation degree on water permeability data pertaining to virtual cement pastes. Standard deviation error bars are given (w/c = 0.4, hydration age: 28 days, particle size range: 1-30 µm). (Li, 2017; Li, et al. 2016)

Consequently, a relatively modest gap should probably be bridged by the nano-packing effect. And that is actually what can be achieved by the presented nano-particle packing-based surface modification method presented in this paper. This can now be realized by slightly reducing the *w/c* ratio as input parameter in the standard porosimetry

methodology briefly sketched in this paper. Expected new information on the C-S-H nano-structure may lead to a specifically designed case of the present set up.

8 Conclusions

In this paper, a DLA model is developed and implemented in a simple low-density, mono-size 2D simulation setup to generate fibrous C-S-H. In contrast to a homogenous material assumed in the traditional vector-based hydration models, C-S-H with fractal structure is closer to the real situation, since this is in conformity with experimental observations. These model investigations yielded a decline in pore size and connected pore fraction, indicating that a thicker C-S-H layer should be taken into account in hydration models.

This information served in an *illustrative* way to upgrade the normal 3D case. Hence, the thickness of the C-S-H layer in this 3D simulation was step-wise enlarged for all particles alike, whereupon the effects on permeability and pore structure were investigated. The size and connectivity of capillary pores declined indeed with the increased thickness of the C-S-H layer, representing less available pore space for fluid transport. As a consequence, also a reduced permeability was observed. The outlined approach would make it possible to bridge the expected modest gap between numerical estimates and experimental permeability results in combination with other involved biases related to the experiments and the actual physical state of the specimens (water saturation degree).

For the same purpose, an alternative approach was designed for which data were available in the literature and obtained by the described porosimetry method. So, an obvious advantage is that it could readily be performed today. Instead of the surface modification approach discussed herein, whereby all particles were provided with a similar rough surfaced layer, the hydrated cement particles were slightly enlarged proportional to their respective sizes (either by way of correcting XIPKM, or by slightly densifying the fresh cement dispersion by DEM). Here the rough surface layer is integrated in the smooth-surfaced layer obtained by XIPKM. It was demonstrated that also in this case, an obvious reduction in permeability is within easy reach.

References

Banthia, N., Mindess, S. Water permeability of cement paste. *Cem. Concr. Res*., 19(1989): 727-736

Bishnoi, S., Scrivener., K.L. μic: A new platform for modelling the hydration of cements. *Cem. Concr. Res*., 39(2009): 266-274

Van Breugel, K. Numerical simulation of hydration and microstructural development in hardening cement-based materials (I) theory. *Cem. Concr. Res*., 25(1995): 319-331; (II) applications. 25(1995): 522-530

Diamond, S. Mercury porosimetry: an inappropriate method for the measurement of pore size distribution in cement-based materials. *Cem. Concr. Res*., 30(2000): 1517-1525

Garboczi, E.J., Bentz, D.P. The effect of statistical fluctuation, finite size error, and digital resolution on the phase percolation and transport properties of the NIST cement hydration model. *Cem. Concr. Res*., 31(10)(2001): 1501-1514.

Garboczi, E.J., Bullard, J.W. Shape analysis of a reference cement. *Cem Concr Res*., 34(2004): 1933-1937.

Gartner, E.M., Kurtis, K.E., Monteiro, P.J.M. Proposed mechanism of C-S-H growth tested by soft X-ray microscopy. *Cem. Concr. Res*., 30(2000): 817-822

Gundersen, H.J.G., Bendtsen, T.F., Korbo, L., *et al*. Some new and efficient stereo-logical methods and their use in pathological research and diagnosis. *Acta Pathol. Microbiol. Immun. Scand*. 96(1988): 379-394

He, H., Guo, Z., Stroeven, P., Stroeven, M., Sluys, LJ. Strategy. Computer simulation of arbitrary-shaped cement grains in concrete. *Im. Anal. Stereol*., 29(2)(2010): 79-84

He, H., Le, L.B.N., Stroeven, P. (2012) "Particulate structure and microstructure evolution of concrete investigated by DEM", Part I. Heron, 57(2):119-132; Part II. *HERON*, 57(2):133-150

Jennings, H.M. A model for the microstructure of calcium silicate hydrate in cement paste. *Cem. Concr. Res*., 30(2000): 101-116

Jennings., H.M. Refinements to colloid model of C-S-H in cement: CM-II. *Cem. Concr. Res*., 38(2008): 275-289

Kameche, Z.A., Ghomari, F., Choinska, M., Khelidj, A. Assessment of liquid water and gas permeabilities of partially saturated ordinary concrete. *Constr. Build. Mater*., 65(2014): 551-565

LaValle, S.M., Kuffner, J.J. Randomized kinodynamic planning, *Int. J. Robot. Res*. 20(2001): 378-400

Le, L.B.N. *Micro-level porosimetry of virtual cementitious materials – Structural impact on mechanical and durability evolution*, Ph.D. Thesis, 2015, Delft University of Technology, Delft, the Netherlands

Le, L.B.N., Stroeven, P. Strength and durability evaluation by DEM approach of green concrete based on gap-graded cement blending. *Adv. Mater. Res*., 450-451(2012): 631-640

Le, L.B.N., Stroeven, M., Sluys, L.J., Stroeven, P. A novel numerical multi-component model for simulating hydration of cement. *Comp. Mater. Sci*., 78(2013): 12-21

Li, K. *Numerical determination of permeability in unsaturated cementitious materials*. Ph.D. Thesis, 2017, Delft University of Technology, Delft, the Netherlands

Li, K., Stroeven, M., Stroeven, P., Sluys, L.J. Investigation of liquid water and gas permeability of partially saturated cement paste by DEM approach. *Cem. Concr. Res*., 83(2016): 104-113

Li, K., Stroeven, P., Stroeven, M., Sluys, L.J. A numerical investigation into the influence of the interfacial transition zone on the permeability of partially saturated cement paste between aggregate surfaces. *Cem. Concr. Res*., 102(2017): 99-108

Li, K., Stroeven, P. RSA vs DEM in view of particle packing-related properties of cementitious materials. *Comp. Concr*., 22(1)(2018): 83-91

Li, K., Stroeven, P. Nano-level C-S-H packing simulation can bridge the gap between experimental and numerical approaches to concrete permeability (to be submitted).

Muller, A.C.A., Scrivener, K.L., Gajewicz, A.M., McDonnald, P.J. Densification of C-S-H measured by 1H NMR relaxometry. *J. Phys. Chem*. C, 117(2013): 403-412

Nguyen, D-T. Micro-indentation creep of Calcium Silicate Hydrate and secondary hydrated cement systems. MSc Thesis, 2014, University of Ottawa, Canada.

O'Connor, R.M. *A distributed discrete element modelling environment – Algorithms, implementations and applications*. PhD Thesis, 1996, MIT, Boston, USA.

Odler, I., Köster, H. Investigation on the structure of fully hydrated cement and tricalcium silicate pastes. III Specific surface area and permeability. *Cem. Concr. Res*., 21(1991): 975-982

Pignat, C., Navi, P., Scrivener, K.L. Simulation of cement paste microstructure hydration, pore space characterization and permeability determination. *Mater. Struct*., 38(2005): 459-466

Rosiwal. A. Űber Geometrische Gesteinsanalysen. Ein einfacher Weg zur ziffermassigen Feststellung des Quantitätsverhaltnisses der Mineral-Bestandteile gemengter Gesteine. *Verh. Kaiserlich-Koeniglichen Geologischen Reichsanstalt*, Vienna, 5/6(1898): 143-175

Stroeven, P. Probing pores by stars - An essential module in porosimetry and permeability estimation methodology of virtual cement paste. *HERON*, 64(3)(2019): 269-296

Stroeven, P., Hu, J. Review paper: Stereology: historical perspective and applicability to concrete technology. *Mat. Struct*. 39(2006): 127-135

Stroeven, P., Hu, J., Stroeven, M. On the usefulness of discrete element computer modeling of particle packing for material characterization in concrete technology. *Comput. Concr*., 6(2009): 133-153

Stroeven, P., Hu, J., Koleva, D.A. Concrete porosimetry: aspects of feasibility, reliability and economy. *Cem. Concr. Comp*. 32(2010): 291-299

Stroeven, P., Le, L.B.N., Sluys, L.J., He, H. Porosimetry by double random multiple tree Structuring. *Im. Anal. Stereol*., 31(2012): 55-63

Stroeven, P., Li, K., Le, L.B.N., He, H. Stroeven, M. Capabilities for property assessment on different levels of the micro-structure of DEM-simulated cementitious materials. *Constr. Build. Mater*., 88(2015): 105-117

Underwood, E.E. *Quantitative stereology*. Addis. Wesley Pub. Co., Cambridge (Mass), 1967.

Williams, S.R., Philipse, A.P. Random packings of spheres and spherocylinders simulated by mechanical contraction. *Phys. Rev*. E 67(2003) (051301):1-9

Ye, G. Percolation of capillary pores in hardening cement pastes. *Cem. Concr. Res*., 35 (2005): 167-176

Zalzale, M., McDonnald, P.J. Scrivener, K.L. A 3D lattice Boltzmann effective media study: understanding the role of C-S-H and water saturation on the permeability of cement paste. *Modelling Simul. Mater. Sci. Eng*., 21(2013): 085016

Zhang, Q., Luo, S.H., Ma, H.C., Wang, X., Qian, J.Z. Simulation on the water flow affected by the shape and density of roughness elements in a single rough fracture *J. Hydrol*., 573(2019): 456-468